Optimal Allocation of Energy Storage Systems for Voltage Control in LV Distribution Networks

Antonio Giannitrapani, *Member, IEEE,* Simone Paoletti, *Member, IEEE,*
Antonio Vicino, *Fellow, IEEE,* Donato Zarrilli

Abstract

This paper addresses the problem of finding the optimal configuration (number, locations and sizes) of energy storage systems (ESSs) in a radial low voltage distribution network with the aim of preventing over- and undervoltages. A heuristic strategy based on voltage sensitivity analysis is proposed to select the most effective locations in the network where to install a given number of ESSs, while circumventing the combinatorial nature of the problem. For fixed ESS locations, the multi-period optimal power flow framework is adopted to formulate the sizing problem, for whose solution convex relaxations based on semidefinite programming are exploited. Uncertainties in the storage sizing decision problem due to stochastic generation and demand, are accounted for by carrying out the optimal sizing over different realizations of the demand and generation profiles, and then taking a worst-case approach to select the ESS sizes. The final choice of the most suitable ESS configuration is done by minimizing a total cost, which takes into account the number of storage devices, their total installed capacity and average network losses. The proposed algorithm is extensively tested on 200 randomly generated radial networks, and successfully applied to a real Italian low voltage network and a modified version of the IEEE 34-bus test feeder.

Index Terms

Energy storage systems, siting and sizing, voltage sensitivity matrix, multi-period optimal power flow.

I. Introduction

PROBLEMS of voltage quality are becoming more and more important in low voltage (LV) distribution networks. Among these, maintaining voltage between specified limits, as required by typical quality of supply standards, is one of the main issues faced by distribution system operators (DSO). This is mostly due to the growing penetration of low carbon technologies, such as distributed generation (DG), electric vehicles and heat pumps, causing modifications of typical power flows in distribution networks. Since peaks of load demand and DG are

The authors are with the Dipartimento di Ingegneria dell'Informazione e Scienze Matematiche, Università degli Studi di Siena, Siena 53100, Italy (e-mail: giannitrapani@dii.unisi.it; paoletti@dii.unisi.it; vicino@dii.unisi.it; zarrilli@dii.unisi.it).

typically not aligned in time, over- and undervoltage conditions may regularly show up. In order to mitigate these problems, several actions can be taken. Grid reinforcement is a possible solution, but in a rapidly evolving scenario as the one distribution networks are now witnessing, deferral of investments in infrastructures could be advisable, and solutions both cheaper and faster to be implemented, should be looked for. In this respect, real and reactive power control of DG, and control of on-load tap changers (OLTC) at secondary substations, are valid alternative solutions proposed in the literature [1]. However, these solutions cannot be always put into practice. On the one hand, depending on both technical and regulatory issues, the DSO might not have control on distributed generators. On the other hand, OLTC control is impracticable when secondary substations are not automated, as is the case in most electricity systems worldwide. In addition, this type of control might have the serious drawback to transmit large disturbances to the medium voltage (MV) network. Very recently, the use of energy storage systems (ESSs) has been investigated to tackle over- and undervoltages [2], [3], [4]. The idea is that an energy storage should play the role of a load in case of overvoltage, and of a generator in case of undervoltage. Pros of the use of ESSs are that voltage problems are solved locally, thus limiting the impact on the MV network, and no curtailment of renewables is required. These advantages add to the well-known general benefits that the use of energy storage brings to the different players (see [5], [6] for general surveys).

Optimal ESS siting and sizing have been addressed in the literature for both transmission and distribution networks, and from the point of view of different power system stakeholders (see, e.g, [7], [8], [9], [10] and references therein). A quite general approach is to formulate the problem in an optimal power flow (OPF) framework, where storage locations and sizes are considered as optimization variables, and a cost function (including, e.g., generation costs, storage installation costs, network losses, etc.) is optimized, subject to power flow constraints and storage dynamics. Since integer variables (used to decide ESS locations) and non-convex power flow constraints make the OPF problems NP-hard, different approaches have been devised to approximate the exact problems and alleviate the computational burden. Linearization via DC approximation is adopted when dealing with transmission networks, where the assumptions underlying DC OPF are typically valid [11], [12], [13], [14]. In [7], the computationally demanding unit commitment (UC) problem over one year to determine optimal storage locations and parameters, is tackled by solving a UC problem for each day of the year separately. When the full AC OPF is considered, as is common for distribution networks, appropriate convex relaxations are often exploited. The second-order cone programming OPF approach of [15] is considered in [16], while convex relaxations based on semidefinite programming (SDP) are used in [17], [18], [19]. Alternating direction method of multipliers is proposed in [4] to break down the original problem into a distributed parallel convex optimization. In [16], [19] convex relaxations are embedded in a mixed integer formulation of the placement problem.

In this paper, we consider the problem of finding the optimal ESS number, locations and sizes with the aim of preventing over- and undervoltages in a radial LV network. We cope with the combinatorial nature of the siting problem by devising a heuristic strategy based on voltage sensitivity analysis. The heuristic determines the locations of a given number of ESSs in the network that are expected to be most effective for voltage support. Then, for fixed storage locations, ESS sizes are determined by formulating a multi-period OPF problem [18], [20], which is tackled

by resorting to SDP convex relaxations [21]. The final choice of the best ESS allocation is done by minimizing a total cost, which takes into account the number of storage devices, their total installed capacity and the average network losses.

Following the taxonomy in [8], the contribution of this paper can be positioned as a mix of heuristic and mathematical programming methods. Its unique feature in the framework of the related literature is the siting procedure, which exploits network topology and line parameters. Advantages of the proposed siting procedure are twofold. First, it is computationally cheap and avoids resorting to a combinatorial formulation involving integer variables. Second, it is specifically designed in order to ease the solution of the subsequent sizing problem by selecting locations with highest sensitivity to solve over- and undervoltages. Similarly to [7], uncertainties in the storage sizing decision problem, mainly arising from stochastic generation and demand, are taken into account by carrying out the optimal sizing for different realizations of demand and generation profiles. For each deployed ESS, the largest size over the considered set of realizations is finally selected. Roughly speaking, this "worst-case" approach is motivated by the attempt to "robustify" the decision by maximizing the probability of feasible storage operation under all possible realizations of demand and generation. Overall, the goal of the proposed procedure is to find a cost-effective ESS installation strategy providing voltage support to the LV network, while keeping the computational burden affordable.

In our framework, the stakeholder is assumed to be the DSO, which faces regularly over- and/or undervoltages in a LV distribution network, and looks for solutions to this issue in order to avoid penalties imposed by the regulatory framework. In this respect, the proposed methodology represents a useful tool to answer the questions "how many", "where" and "how much," thus supporting the decision making at the planning level. Consequently, ESSs are assumed to be installed and operated by the DSO, i.e. they are not integrated in households or DG plants out of the control of the DSO. Operation of installed ESSs can be accomplished by adapting any of the control policies and techniques proposed in the literature to this aim, see, e.g., [2], [18], [22].

Applications presented in the paper (a real Italian LV network, a modified version of the IEEE 34-bus test feeder, and 200 randomly generated radial networks) provide encouraging results when our ESS allocation strategy is compared with exhaustive search. Moreover, they bring interesting insights in how the network topology, and historical load demand and DG profiles, can be exploited to identify the most suitable candidate buses for ESS siting.

The paper is organized as follows. Section II presents the network model and the problem formulation. The sizing problem is addressed in Section III, whereas the proposed heuristic for ESS siting is described in Section IV. Numerical results are reported and discussed in Section V. Finally, conclusions are drawn in Section VI. A preliminary version of this work was presented in [23].

II. Network Model and Problem Formulation

We consider LV distribution networks with radial layout, that are frequent in LV public distribution systems of many countries worldwide. The network model is described in this section, including equations and constraints

characterizing loads, distributed generators and storage units connected to the network.

Consider a radial LV network described by a tree $(\mathcal{N}, \mathcal{E})$, where $\mathcal{N} = \{1, 2, \dots, n\}$ is the set of nodes (*buses*) and $\mathcal{E}$ is the set of edges (*lines*). The admittance-to-ground at bus i is denoted by y_{ii}. The line admittance between nodes i and j is denoted by y_{ij} and satisfies $y_{ij} = y_{ji}$. If $(i, j) \notin \mathcal{E}$, i.e. buses i and j are not connected by a line, $y_{ij} = 0$. The network admittance matrix $Y = [Y_{ij}] \in \mathbb{C}^{n \times n}$ is a symmetric matrix defined as

$$Y_{ij} = \begin{cases} y_{ii} + \sum_{h \neq i} y_{ih} & \text{if } i = j \\ -y_{ij} & \text{otherwise.} \end{cases} \tag{1}$$

Consider discrete time steps indexed by $t = 1, 2, \dots$. The complex voltage and current injection at bus k and time t are denoted by $V_k(t)$ and $I_k(t)$, while $P_k(t)$ and $Q_k(t)$ denote the corresponding active and reactive power injections. The power balance equation at bus k and time t reads as

$$P_k(t) + \jmath Q_k(t) = V_k(t) I_k^*(t) = V_k(t) \sum_{j=1}^{n} V_j^*(t) Y_{kj}^*, \tag{2}$$

where $\jmath$ is the unit imaginary number, $(\cdot)^*$ denotes the complex conjugate operator and $I_k(t) = \sum_{j=1}^{n} Y_{kj} V_j(t)$.

Bus 1 is assumed to be the slack bus, representing the interconnection with the MV network. The slack bus is characterized by fixed voltage magnitude and phase, i.e. $V_1(t)$ is known for all t. Conversely, complex voltages $V_k(t)$ at buses $k \in \mathcal{N}^L = \{2, \dots, n\}$ are free variables of the power flow problem. For them, voltage quality requirements impose the magnitude to remain within specified limits, i.e.

$$\underline{v}_k^2 \leq |V_k(t)|^2 \leq \overline{v}_k^2, \tag{3}$$

where $\underline{v}_k \leq \overline{v}_k$ are given bounds. Limitations on the transmission line capacities are also imposed by requiring the real power flow from bus i to bus j to be bounded, i.e.

$$P_{ij}(t) \leq \overline{P}_{ij}, \tag{4}$$

where $P_{ij}(t) = \mathrm{Re}\left(V_i(t)\left[V_i(t) - V_j(t)\right]^* y_{ij}^*\right)$ is the real power transferred from bus i to bus j at time t and $\overline{P}_{ij} = \overline{P}_{ji}$ is a given upper bound depending only on the physical properties of the line [24].

The set of buses equipped with ESS is denoted by $\mathcal{S} \subseteq \mathcal{N}^L$. For $s \in \mathcal{S}$, let $e_s(t)$ be the storage energy level at bus s and time t. The dynamics of $e_s(t)$ is modelled by the following first-order difference equation:

$$e_s(t+1) = e_s(t) + r_s(t)\Delta t, \tag{5}$$

where $r_s(t)$ is the average active power exchanged with the storage unit at time t, and Δt is the time step. Note that $r_s(t)$ can take both positive and negative values (charging and discharging, respectively). The initial condition for the storage energy level is assumed to be known:

$$e_s(1) = e_s^1. \tag{6}$$

Moreover, both $r_s(t)$ and $e_s(t)$ are bounded as follows:

$$-\underline{R}_s \leq \quad r_s(t) \quad \leq \overline{R}_s \tag{7}$$

$$0 \leq \quad e_s(t) \quad \leq E_s, \tag{8}$$

where $\underline{R}_s$, $\overline{R}_s > 0$ are the ramp rate limits and E_s is the storage capacity installed at bus s. Similarly to (7), bounds $\underline{B}_s < \overline{B}_s$ can be imposed on the average reactive power $b_s(t)$ exchanged with the ESS:

$$\underline{B}_s \leq b_s(t) \leq \overline{B}_s. \tag{9}$$

Let $P_k^D(t)$ and $Q_k^D(t)$ denote the active and reactive power demand at bus k and time t. Similarly, the active and reactive power generation at bus k and time t are denoted by $P_k^G(t)$ and $Q_k^G(t)$. For a generic bus $k \in \mathcal{N}^L$ having loads, generators and storage units connected to it, the active and reactive power injections $P_k(t)$ and $Q_k(t)$ take the general expressions:

$$P_k(t) = P_k^G(t) - P_k^D(t) - r_k(t) \tag{10}$$

$$Q_k(t) = Q_k^G(t) - Q_k^D(t) - b_k(t). \tag{11}$$

The following additional constraints apply to buses not equipped with ESS:

$$r_h(t) = b_h(t) = 0, \quad h \in \mathcal{N}^L \backslash \mathcal{S}. \tag{12}$$

The quantities $P_k^D(t)$, $Q_k^D(t)$, $P_k^G(t)$ and $Q_k^G(t)$ are considered as known inputs in (10) and (11). Recall that generators in LV networks are mostly of PV and micro-wind type. These small generators are typically connected to the network through grid-tie inverters. High-quality modern grid-tie inverters feature a fixed power factor close to 1, so that $Q_k^G(t) \simeq 0$. This justifies the fact that, except for the slack bus, buses with generation are treated in this paper as load buses[1]. In case no load or generator is connected to bus $k \in \mathcal{N}^L$, the corresponding demand or generation are assumed to be zero.

The deployment cost of distributed storage systems in the grid depends both on the number of devices (e.g., costs incurred for installation and maintenance) and the total amount of energy storage capacity installed. Moreover, the effectiveness of a given ESS in providing voltage support can vary significantly, depending on the bus to which it is connected. Hence, the following problem needs to be tackled at the planning stage.

Problem 1: Find the minimum-cost ESS *number*, *locations* and *sizes* for preventing over- and undervoltages in the considered LV network.

In other words, one has to decide the cardinality and the composition of the set of ESS locations $\mathcal{S}$, as well as the storage capacities E_s for all $s \in \mathcal{S}$. Solving Problem 1 is a formidable task, involving a multi-period OPF with mixed binary and continuous optimization variables. In order to circumvent the combinatorial nature of the problem and reduce its computational complexity, a two-step, iterative procedure is hereafter proposed. For a given number of ESSs, a heuristic based on voltage sensitivity analysis, which explicitly takes into account the network topology, is devised in order to select the most effective ESS locations for voltage support. Then, the size of each ESS is determined by solving a multi-period OPF problem. These steps are iterated for different numbers of ESSs,

[1]In the power flow literature, generator buses would be typically characterized by the fact that generated active power and voltage magnitude are prespecified, while generated reactive power and voltage phase are determined by the network state.

in order to minimize the overall deployment cost. Each step of the proposed ESS allocation procedure is illustrated separately in the following sections.

III. Storage Sizing

Assume that the set $\mathcal{S}$ is given, i.e. the ESS number and locations in the network have been decided. The considered storage sizing problem aims at finding the minimum total storage capacity making it possible to satisfy the voltage constraints (3) over a discrete time horizon $\mathcal{T}$. Typically, $\mathcal{T}$ spans one day or one week, in order to account for the periodicity of demand and generation profiles. Optimization variables in this problem are the storage size E_s and the real and reactive power $r_s(t)$ and $b_s(t)$ exchanged with each ESS, $t \in \mathcal{T}$, in addition to the typical OPF optimization variables. Conversely, demand and generation profiles are given, e.g., they are extracted from a historical data set.

In order to take into account line losses, which are of primary interest in LV networks, we define the cost function

$$J(C_S, C_L) = C_L + \gamma C_S, \tag{13}$$

where $C_S = \sum_{s\in\mathcal{S}} E_s$ [kWh] is the total installed storage capacity, $C_L = \frac{1}{|\mathcal{T}|}\sum_{t\in\mathcal{T}}\sum_{k\in\mathcal{N}} P_k(t)\Delta t$ [kWh] represents the average total line losses per sampling time, $|\mathcal{T}|$ denotes the cardinality of the set $\mathcal{T}$ and $\gamma \geq 0$ is a weighting parameter. Then, the considered multi-period OPF problem for storage sizing reads as

$$\begin{aligned} &\min_{V_k(t), r_s(t), b_s(t), Es} J(C_S, C_L) \\ &\text{s. t.} \quad (2)-(12), \quad k \in \mathcal{N}^L,\ s \in \mathcal{S},\ (i,j) \in \mathcal{E},\ t \in \mathcal{T}. \end{aligned} \tag{14}$$

Notice that, according to (2), active power injections $P_k(t)$ needed to evaluate C_L in (13) can be replaced with $\mathrm{Re}\left(V_k(t)\sum_{j=1}^{n} V_j^*(t) Y_{kj}^*\right)$, where $\mathrm{Re}(\cdot)$ denotes the real part of a complex number. Unfortunately, problem (14) is non-convex and therefore hard to solve. A common approach to reduce the computational burden is to compute an approximated solution by resorting to SDP convex relaxations. To this aim, denote by ϵ_k the kth standard basis vector of R^n, and define

$$\mathbf{M}_k = \begin{bmatrix} \epsilon_k\epsilon_k^T & 0 \\ 0 & \epsilon_k\epsilon_k^T \end{bmatrix} \tag{15}$$

$$\mathcal{Y}_k = \epsilon_k\epsilon_k^T Y \tag{16}$$

$$\mathbf{Y}_k = \frac{1}{2}\begin{bmatrix} \mathrm{Re}\left(\mathcal{Y}_k + \mathcal{Y}_k^T\right) & \mathrm{Im}\left(\mathcal{Y}_k^T - \mathcal{Y}_k\right) \\ \mathrm{Im}\left(\mathcal{Y}_k - \mathcal{Y}_k^T\right) & \mathrm{Re}\left(\mathcal{Y}_k + \mathcal{Y}_k^T\right) \end{bmatrix} \tag{17}$$

$$\overline{\mathbf{Y}}_k = \frac{-1}{2}\begin{bmatrix} \mathrm{Im}\left(\mathcal{Y}_k + \mathcal{Y}_k^T\right) & \mathrm{Re}\left(\mathcal{Y}_k - \mathcal{Y}_k^T\right) \\ \mathrm{Re}\left(\mathcal{Y}_k^T - \mathcal{Y}_k\right) & \mathrm{Im}\left(\mathcal{Y}_k + \mathcal{Y}_k^T\right) \end{bmatrix} \tag{18}$$

$$\mathcal{Y}_{ij} = y_{ij}\epsilon_i(\epsilon_i - \epsilon_j)^T \tag{19}$$

$$\mathbf{Y}_{ij} = \frac{1}{2}\begin{bmatrix} \mathrm{Re}\left(\mathcal{Y}_{ij} + \mathcal{Y}_{ij}^T\right) & \mathrm{Im}\left(\mathcal{Y}_{ij}^T - \mathcal{Y}_{ij}\right) \\ \mathrm{Im}\left(\mathcal{Y}_{ij} - \mathcal{Y}_{ij}^T\right) & \mathrm{Re}\left(\mathcal{Y}_{ij} + \mathcal{Y}_{ij}^T\right) \end{bmatrix}, \tag{20}$$

where $(\cdot)^T$ denotes the transpose operator of a matrix and $\mathrm{Im}(\cdot)$ is the imaginary part of a complex number. Moreover, define the rank-1 matrix $W(t) = U(t)U(t)^T$, where $U(t) = \left[\ \mathrm{Re}\left(V(t)\right)^T\ \mathrm{Im}\left(V(t)\right)^T\ \right]^T$ and $V(t) = [\ V_1(t)\ \ldots\ V_n(t)\ ]^T$. By taking the real and imaginary parts of (2), the active and reactive power balance equations at bus k and time t can be rewritten as

$$\mathrm{tr}\left(\mathbf{Y}_k W(t)\right) = P_k(t) \tag{21}$$

$$\mathrm{tr}\left(\overline{\mathbf{Y}}_k W(t)\right) = Q_k(t), \tag{22}$$

where $\mathrm{tr}(X)$ is the trace of the square matrix X. Similarly, it can be shown that (3) is equivalent to

$$\underline{v}_k^2 \leq \mathrm{tr}\left(\mathbf{M}_k W(t)\right) \leq \overline{v}_k^2 \tag{23}$$

and (4) is equivalent to

$$\mathrm{tr}\left(\mathbf{Y}_{ij} W(t)\right) \leq \overline{P}_{ij}. \tag{24}$$

The interested reader is referred to [24, Lemma 1] for a detailed derivation of (21)-(24). Adding all together, a convex relaxation of problem (14) takes the form

$$J^* = \min_{W(t), r_s(t), b_s(t), E_s} J(C_S, C_L) \tag{25a}$$

s. t.

$$\mathrm{tr}\left(\mathbf{Y}_k W(t)\right) = P_k^G(t) - P_k^D(t) - r_k(t) \tag{25b}$$

$$\mathrm{tr}\left(\overline{\mathbf{Y}}_k W(t)\right) = Q_k^G(t) - Q_k^D(t) - b_k(t) \tag{25c}$$

$$\underline{v}_k^2 \leq \mathrm{tr}\left(\mathbf{M}_k W(t)\right) \leq \overline{v}_k^2 \tag{25d}$$

$$\mathrm{tr}\left(\mathbf{Y}_{ij} W(t)\right) \leq \overline{P}_{ij} \tag{25e}$$

$$e_s(t+1) = e_s(t) + r_s(t)\Delta t \tag{25f}$$

$$e_s(1) = e_s^1 \tag{25g}$$

$$-\underline{R}_s \leq r_s(t) \leq \overline{R}_s \tag{25h}$$

$$0 \leq e_s(t) \leq E_s \tag{25i}$$

$$\underline{B}_s \leq b_s(t) \leq \overline{B}_s \tag{25j}$$

$$r_h(t) = b_h(t) = 0, \quad h \in \mathcal{N}^L \setminus \mathcal{S} \tag{25k}$$

$$W(t) \succeq 0 \tag{25l}$$

$$k \in \mathcal{N}^L,\ s \in \mathcal{S},\ (i,j) \in \mathcal{E},\ t \in \mathcal{T},$$

where $X \succeq 0$ means that the symmetric matrix X is positive semidefinite. In problem (25), constraints (25b) and (25c) express the power balance equation (2) with $P_k(t)$ and $Q_k(t)$ given by (10) and (11), constraints (25d) and (25e) impose voltage and line capacity limits (3) and (4), respectively, constraints (25f)-(25j) model the storage

dynamics (5)-(9) and, finally, (25l) is a technical constraint deriving from the transformation of variables from $V(t)$ to $W(t)$. Notice that problem (25) can be made equivalent to the original problem (14) by adding the additional non-convex constraint $\mathrm{rank}\left(W(t)\right) = 1$ (see, e.g., [21], [24]).

Remark 1: Although problem (25) is formulated in a deterministic framework, in a real context demand and generation are affected by uncertainty. This can be modeled by considering the data in each time horizon $\mathcal{T}$ as a sample of the cyclostationary stochastic process involving both renewables and loads. In this respect, the optimal cost J^*, as well as the optimal ESS sizes E_s^*, are also stochastic quantities, since the cost function (25a) depends on the particular realization of demand and generation profiles over the considered time horizon. In order to guarantee feasibility of problem (25), the size of the sth ESS should be selected as the largest E_s^*, taken with respect to all possible realizations of demand and generation profiles. When historical data are available, a viable approach is to solve problem (25) separately for each sample in the data set, and then size each ESS according to the largest capacity found. Formally, let $E_s^{*,d}$ denote the optimal size of the sth ESS for the demand and generation profiles of sample $d = 1, \ldots, D$. Then, its final size $\hat{E}_s^*$ is selected as

$$\hat{E}_s^* = \max_{d=1,\ldots,D} E_s^{*,d}. \tag{26}$$

In this study, the time horizon $\mathcal{T}$ of a sample is assumed to cover one day. In order to link coherently consecutive days, the additional constraint stating that the storage energy level at the beginning of a day equals that at the end of the day, namely

$$\sum_{t \in \mathcal{T}} r_s(t) = 0, \quad \forall s \in \mathcal{S}, \tag{27}$$

is added in (25).

Remark 2: If needed, the ramp rate limits $\underline{R}_s$ and $\overline{R}_s$ can be made dependent on the ESS size E_s by replacing (7) and (25h) with

$$-\underline{\rho}_s E_s \leq r_s(t) \leq \overline{\rho}_s E_s, \tag{28}$$

for fixed positive constants $\underline{\rho}_s$ and $\overline{\rho}_s$. Since (28) is convex, this extension does not change the computational complexity of the optimization problem (25).

IV. Storage Siting

In this section, we propose a procedure for finding a suitable placement of a given number of ESSs in a radial distribution network, based on Clustering and Sensitivity Analysis (CSA). The underlying idea consists of partitioning the network into n_C disjoint subnetworks, and then selecting the most appropriate bus within each subnetwork where to deploy an ESS. An outline of the CSA algorithm is presented below.

CSA Algorithm

1) *Network clustering.* First, the set $\mathcal{N}^L$ is partitioned into n_C disjoint subsets. To this aim, a clustering algorithm is run on an auxiliary weighted graph, consisting of a complete graph built over $\mathcal{N}^L$. The weight associated

to the edge (h,k) is equal to the (h,k)-entry of the *voltage sensitivity matrix* $\Psi \in \mathbb{R}^{(n-1)\times(n-1)}$ (see, e.g., [25]):

$$\Psi_{hk} = \partial|V_k|/\partial P_h, \quad h,k \in \mathcal{N}^L. \tag{29}$$

The value Ψ_{hk} is a measure of how much the voltage at bus k is sensitive to active power injection at bus h. The effect of reactive power injection Q_h on bus voltages is neglected since $\partial|V_k|/\partial Q_h \ll \partial|V_k|/\partial P_h$ in LV networks. Among several methods for graph clustering available in the literature (see, e.g., [26]), the algorithm adopted in our procedure is based on [27]. It searches for n_C subgraphs which form a partition of the original graph, while minimizing the sum of the weights associated to the removed edges. In our setting, this amounts to constructing the partition of the auxiliary graph in order to minimize the sum of the voltage sensitivities associated to the removed connections. This means that a pair of buses with high mutual voltage sensitivity are likely to end up in the same subset. The outcome of the clustering algorithm is a partition $\mathcal{N}_i$, $i = 1,\dots,n_C$, of the node set $\mathcal{N}^L$, from which subnetworks $\Upsilon_i = (\mathcal{N}_i, \mathcal{E}_i)$ are reconstructed by defining $\mathcal{E}_i = \{(h_i,k_i) \in \mathcal{E} \ : \ h_i \in \mathcal{N}_i, k_i \in \mathcal{N}_i\}$.

2) *Candidate buses*. For each subnetwork Υ_i, $i = 1,\dots,n_C$, the *critical buses* are identified as the buses with generation and the buses that are leaves of the original network. Then, the set Ω_i of *candidate buses* is formed with all the buses along the paths connecting any pair of critical buses of Υ_i.

3) *Bus selection.* The criterion according to which the most suitable bus among all candidate buses is selected, exploits the voltage sensitivities (29) again. The ESS for subnetwork i is placed at the node

$$k_i^* = \arg\max_{k_i \in \Omega_i} \min_{h_i \in \mathcal{N}_i \setminus \{k_i\}} \Psi_{h_i k_i}. \tag{30}$$

This choice aims at maximizing the controllability of the voltage in the subnetwork.

The rationale behind the CSA algorithm is to exploit the voltage sensitivity matrix in order to determine the best ESS locations. Indeed, the voltage sensitivity matrix helps identify the most effective connections among buses with the aim of maximizing the effect of power injection on voltage variation. Clearly, if a subnetwork Υ_i resulting from step 1) does not contain any bus affected by voltage problems, Υ_i can be safely left without ESS, thus skipping steps 2) and 3) of the procedure for that subnetwork.

The parameter n_C, which is an upper bound to the final number of ESSs to be deployed, is an input to the CSA algorithm and must be selected by trading-off fixed and variable costs of storage deployment. A small number of ESSs results in smaller installation and maintenance costs, but typically requires a larger total capacity to be installed in order to face all possible network operating conditions with fewer ESSs. In this respect, a possible selection strategy for the number of subnetworks is to repeat the CSA algorithm for increasing values of n_C, find the optimal size of each ESS by solving problem (25), and then evaluate the corresponding total deployment cost as

$$C_T(n_C) = c_f \, n_S + c_v \, \mathbf{E}[J^*], \tag{31}$$

where $n_S \leq n_C$ is the number of ESSs resulting from running the CSA algorithm with n_C clusters, J^* is the

Algorithm 1 Summary of the ESS allocation procedure

for $i = 1$ **to** $n - 1$ **do**

$\mathcal{S}(i) \leftarrow$ run the CSA algorithm with $n_C = i$

for $d = 1$ **to** D **do**

$(E_s^{*,d}, J^{*,d}) \leftarrow$ solve problem (25) with $\mathcal{S} = \mathcal{S}(i)$

end for

$\hat{E}_s^*(i) \leftarrow$ evaluate (26), $s \in \mathcal{S}(i)$

$C_T(i) \leftarrow$ evaluate (31)

end for

$i^* = \arg\min_i C_T(i)$

place ESSs at $\mathcal{S}(i^*)$ with sizes $\hat{E}_s^*(i^*)$

optimal cost of problem (25), c_f accounts for the fixed costs related to a single ESS and c_v is the unitary cost associated with J^*. Expectation $\mathbf{E}[\cdot]$ is taken with respect to demand and generation probability distributions. In fact, J^* is a random variable as explained in Remark 1. In practice, the expected value $\mathbf{E}[J^*]$ is replaced with the sample mean $\bar{J}^*$ computed over the available data set. Formally, let $J^{*,d}$ be the optimal cost of problem (25) for the demand and generation profiles of sample $d = 1, \ldots, D$, then

$$\bar{J}^* = \frac{1}{D} \sum_{d=1}^{D} J^{*,d}. \tag{32}$$

Remark 3: Since the voltage sensitivity matrix Ψ cannot be computed analytically, it is estimated numerically. This is done by evaluating the voltage variation at bus k after a unit power injection at bus h, which amounts to solving a load flow problem. While it is true that the entries of (29) do depend on the particular demand and generation profiles, it turns out that their variation is negligible even when very different profiles are considered. This confirms that Ψ is determined mostly by the network topology and admittances of the lines, as already observed in previous works [2], [25]. By virtue of this observation, matrix Ψ is computed only once, by considering the average demand and generation profiles. The same matrix is then used for solving points 1) and 3) of the CSA algorithm, irrespective of the number of clusters selected.

The overall ESS allocation procedure is summarized in Algorithm 1. The CSA algorithm for ESS siting is quite inexpensive. In fact, the hardest task of the CSA algorithm is the network clustering (step CSA.1), which is however carried out in few seconds for networks including up to a hundred buses (on a 2.4 GHz single-core CPU). The overall computational burden of the procedure is dictated by the solution of the sizing problem. Due to the time correlation introduced by the presence of ESSs, it is necessary to solve a multi-period OPF. Moreover, the full AC OPF needs to be solved since LV networks are considered. In this respect, the adopted SDP approximation yields a significant complexity reduction. Nevertheless, since the solution of the multi-period OPF is repeated for all the days in the historical data set, this task is by far the most time consuming one. Parallel implementation of this step

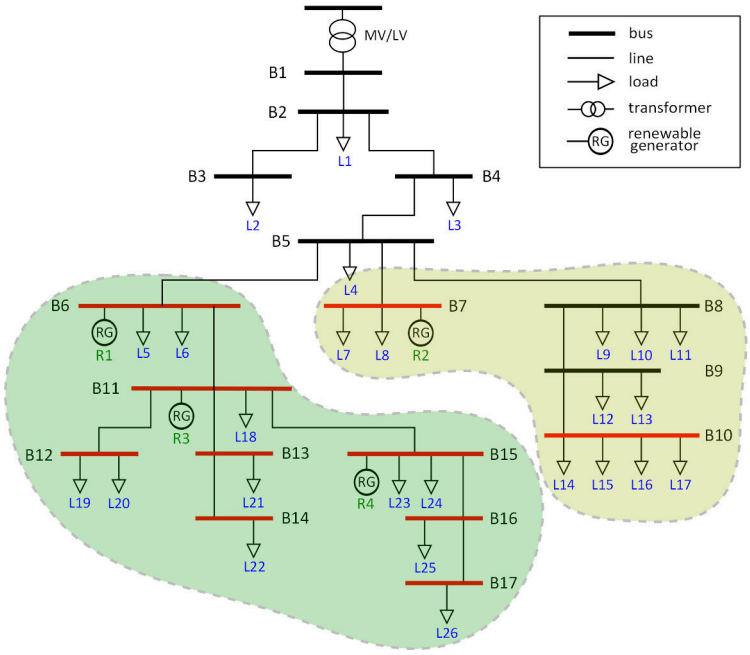

Fig. 1. Topology of the IT-LV network and output of the CSA algorithm for $n_C = 6$. Two clusters (highlighted in green and yellow) contain a nonempty set of candidate buses (red bars). The remaining four clusters are singletons, none of which is a candidate bus.

could be effective in reducing the overall computation time.

V. Numerical Results

The strategy for ESS siting and sizing described so far, is demonstrated on several case studies in this section.

The first application considers a real LV network, provided by the main Italian DSO (see Fig. 1), and denoted by IT-LV in the following. The network consists of 17 buses, hosting 26 loads and 4 PV units. A total of 9 leaf and generation buses are present. Among them, only 8 critical buses are retained since leaf node 3 does not experience any voltage problem. For all loads and generators, four months (120 days) of active and reactive power profiles are available with time step $\Delta t = 15$ min. These profiles are perturbed to originate both over- and undervoltages. This means that, in the absence of storage units installed in the network, voltage magnitudes violate the voltage quality constraints (3) at certain buses and time steps.

The second case study refers to a modified version of the IEEE 34-bus test feeder [28]. Two PV units are installed at buses 7 and 19, resulting in a total of 11 critical buses. Four daily demand and generation profiles, representative of different operating conditions, are simulated with time step $\Delta t = 15$ min.

In the third case study, the CSA algorithm is tested on 200 randomly generated radial networks. The objective of the experiment is to evaluate the optimality gap of the solutions provided by the CSA algorithm. For this reason, the test is carried out for problem sizes making it possible to determine the optimal ESS siting via exhaustive search.

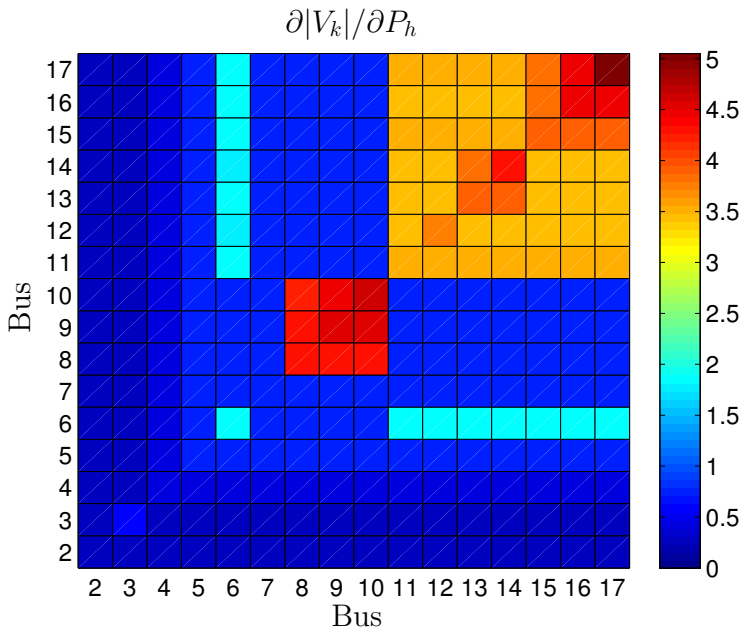

Fig. 2. Graphical representation of the voltage sensitivity matrix Ψ for the IT-LV network.

A. Simulation Setup

For all buses $k \in \mathcal{N}^L$, in accordance with the European Norm 50160, a 10% tolerance around the nominal voltage magnitude is allowed in both directions, i.e. $\underline{v}_k = 0.9$ pu and $\overline{v}_k = 1.1$ pu in (3). The bounds $\overline{P}_{ij}$ in (4) are all set to 35 kW. The ESS technology adopted for the simulations features the following parameters. Active ramp limits in (7) are chosen such that $\overline{R}_k = \underline{R}_k = 25$ kW, and the bounds $\underline{B}_k$ and $\overline{B}_k$ in (9) are set to keep the angle shift between -10 and +10 deg. An empty initial storage level (6) is assumed for all ESSs, i.e. $e_k^1 = 0$ kWh. The weighting parameter in (13) is set to $\gamma = 2.5 \cdot 10^{-3}$ (a discussion of this choice for the IT-LV network is presented in Section V-C), whereas $c_f = 10$ k€ and $c_v = 575$ €/kWh are chosen in the total deployment cost (31). All the results presented hereafter are obtained by using the CVX modelling toolbox [29] and the SeDuMi solver [30].

B. ESS Siting

For the IT-LV network, the voltage sensitivity matrix Ψ defined in (29) is computed numerically as described in Remark 3. A pseudocolor plot of Ψ is shown in Fig. 2. This kind of representation is useful to visualize the effect that a power injection at a given bus has on the voltage at the other buses. Cells with warmer colors denote strongly connected pairs of buses, whereas cells filled with colder colors correspond to weakly coupled buses.

For a given number of clusters n_C, the CSA algorithm returns a suitable number n_S of ESSs to be installed, as well as their locations in the network. The results obtained for the case $n_C = 6$ are shown in Fig 1. The procedure terminates with $n_S = 2$ storage units, allocated at buses 7 and 11.

The CSA algorithm is repeated for all possible values of n_C, ranging from 1 to 16. It turns out that, irrespective

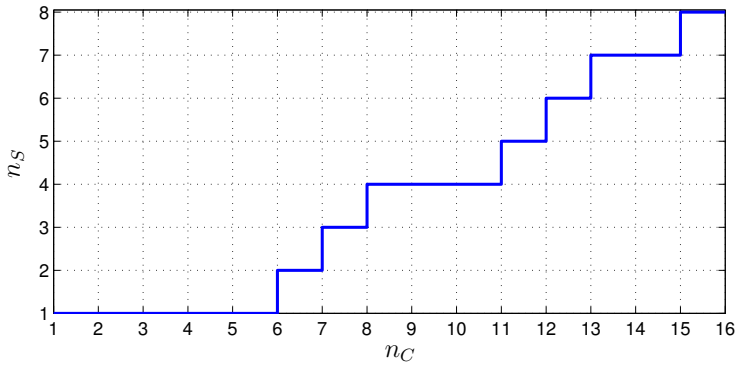

Fig. 3. Number of ESSs n_S returned by the CSA algorithm as a function of the number of clusters n_C for the IT-LV network.

of the number of clusters, storage units are always placed at critical buses as defined in Section IV. The number n_S of ESSs to be deployed as a function of the number of clusters n_C is shown in Fig. 3. It can be observed that n_S is typically strictly less than n_C. In the limit case in which each bus forms a different cluster (i.e. $n_C = 16$), the CSA algorithm returns $n_S = 8$, corresponding to the 8 critical buses present in the network. This confirms that such buses represent preferred locations in which to deploy ESSs, thus supporting the intuition which is at the basis of the CSA algorithm.

In order to assess the effectiveness of the siting procedure, the CSA algorithm is tested under four typical operating conditions of the original LV network (without ESSs):

NV – neither over- nor undervoltages at any bus;

UV – only undervoltages at some buses;

OV – only overvoltages at some buses;

UOV – both over- and undervoltages at some buses.

For each of the four scenarios, a representative day is extracted from the data set and the corresponding demand and generation profiles are considered. The CSA algorithm is run with $n_C = 6, 7, 8$, resulting in $n_S = 2, 3, 4$ storage units, respectively (see Fig. 3). Then, problem (25) is solved by assuming ESSs installed at the buses returned by

TABLE I

PERFORMANCE EVALUATION OF THE CSA ALGORITHM FOR THE IT-LV NETWORK (J^*_{CSA}/J^*_{OPT}).

n_S	NV	UV	OV	UOV
2	1.008	1.057	1.022	1.000
3	1.001	1.000	1.038	1.000
4	1.006	1.008	1.000	1.000

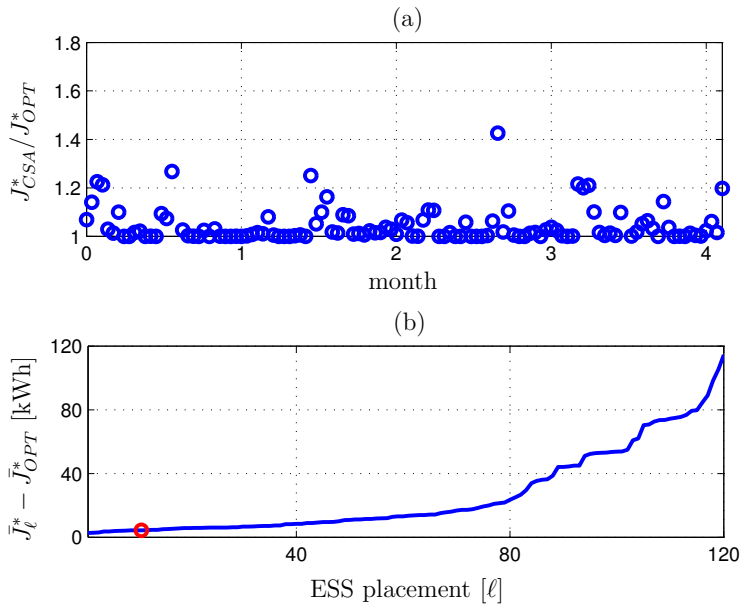

Fig. 4. Validation of the CSA algorithm for $n_S = 2$ on the IT-LV network. (a) Ratio J^*_{CSA}/J^*_{OPT} for all the four months in the data set. (b) Average optimality gap $\bar{J}^*_\ell - \bar{J}^*_{OPT}$ for all 120 possible placements of two ESSs in the network (sorted in increasing order). The ESS placement provided by the CSA algorithm ranks #11 (red dot).

the siting procedure. Denote by J^*_{CSA} the corresponding optimal cost in (25). Such a quantity is compared with the optimal cost J^*_{OPT}, computed over all possible placements of n_S ESSs in the network (e.g., for $n_S = 2$, 120 different ESS placements have to be considered). The ratio J^*_{CSA}/J^*_{OPT} is a measure of the performance degradation which is incurred when using the CSA algorithm for ESS siting (see Table I). The increase in the cost ranges from zero (UOV scenario) to 5.7% (UV scenario and $n_S = 2$). In particular, for the day when both over- and undervoltages are experienced, the ESS locations returned by the CSA algorithm are optimal. Conversely, for the day featuring only undervoltages, the placement determined by the CSA algorithm for two ESSs implies a cost J^*_{CSA} which is 5.7% higher than the optimal one J^*_{OPT}. Notice, however, that the optimal ESS placement (i.e. the one yielding the optimal cost J^*_{OPT}), being in general different from day to day, is not physically realizable. This means that, for fixed n_S, there does not exist any placement of n_S ESSs yielding the optimal cost J^*_{OPT} for all the four days. In this respect, the solution provided by the CSA algorithm turns out to be a good trade-off among different operating conditions and performs quite well in all scenarios. Moreover, the computation of the optimal placement requires an exhaustive search among all possible placements of n_S storage units. This is a very time-consuming task which becomes rapidly intractable as n_S grows. On a 2.4 GHz single-core CPU, it takes about 16 hours to compute the first row of Table I, while it takes more than 10 days to compute the third one.

A more extensive numerical validation of the CSA algorithm is carried out for the case $n_S = 2$. The same quantity reported in Table I is computed for all the 120 days available in the data set. The results, shown in Fig. 4(a), confirm the good performance of the CSA algorithm under every operating condition. Indeed, the few days for which the

cost increase is above 10%, correspond to days experiencing undervoltages and for which *ad hoc* ESS placements result in a quite lower optimal cost J^*_{OPT}. However, the satisfactory behavior of the CSA algorithm on average can be appreciated by comparing the sample means $\bar{J}^*_{OPT}$ and $\bar{J}^*_{CSA}$, computed by averaging J^*_{OPT} and J^*_{CSA} over the 120 days. Specifically, we obtain $\bar{J}^*_{OPT} = 151$ kWh and $\bar{J}^*_{CSA} = 156$ kWh, resulting in an average performance degradation of 3.5%. Figure 4(b) shows the daily optimality gap averaged over the whole data set, namely the quantity $\bar{J}^*_\ell - \bar{J}^*_{OPT}$, for all possible placements of two ESSs in the network, indexed by $\ell = 1, \ldots, 120$. It turns out that the solution provided by the CSA algorithm ranks #11, with an average optimality gap very close to that of the best ESS placement (namely, buses 10 and 11 for these network and data set).

C. ESS Sizing

Once the CSA algorithm has returned the number and locations of ESSs to be deployed, the size of each storage unit is determined by solving problem (25) for each day in the data set and then applying (26).

An aspect to be considered is the quality of the solution found by solving (25). Recall that (25) is a convex relaxation of the original non-convex problem (14), obtained by neglecting the rank-1 constraint. Feasibility and optimality of the solution of the relaxed problem for the original one are guaranteed if $\mathrm{rank}\,\big(W(t)\big) = 1$ for all $t \in \mathcal{T}$. For the IT-LV network and the corresponding data set, the rank-1 constraint is never satisfied. Nevertheless, by solving a load flow problem with the ESS power exchange profiles $r_s(t)$ and $b_s(t)$ resulting from (25) with $\gamma = 2.5 \cdot 10^{-3}$, the solution of the relaxed problem turns out to be always feasible for (14), i.e. no violations of the constraints occur. Indeed, the ratio of the second to the first singular value of matrix W, namely $\sigma_2(W)/\sigma_1(W)$, is of the order of 10^{-11} with the choice $\gamma = 2.5 \cdot 10^{-3}$, i.e. matrix W is *almost* rank-1.

The parameter γ in (13) represents the weight assigned to the total storage capacity term C_S with respect to the line loss term C_L in the cost function J. In order to tune it properly, several tests have been performed by considering demand and generation profiles over a challenging day present in the data set, i.e. a day featuring both over- and undervoltages in the absence of ESSs. The values of the terms C_S and C_L at the optimum of problem (25) are shown as a function of γ in Fig. 5. As expected, larger values of γ yield solutions with smaller total installed ESS capacity, whereas smaller values of γ result in smaller line losses. Moreover, it can be observed that, as the weight γ increases, C_S cannot decrease below a lower bound in order to ensure feasibility of the voltage constraints in the optimization problem. Consequently, as C_S tends to its lower bound, C_L approaches a constant value as well. The choice $\gamma = 2.5 \cdot 10^{-3}$ guarantees a total storage capacity C_S as small as possible. Notice that γ also affects the quality of the solution of the relaxed problem. For large values of γ, it turns out that the solution of (25) is no longer feasible for the original problem (14). The reason for this can be understood by looking at the ratio $\sigma_2(W)/\sigma_1(W)$ in Fig. 6, which becomes non-negligible for $\gamma > 9 \cdot 10^{-3}$.

The total deployment cost (31) as a function of the number of ESSs is shown in Fig. 7(a). All the 120 days of the available data set are considered at this stage. For some ESS placements, there may exist days in the data set for which the original problem (14) does not admit a solution. For instance, this may occur when too few ESSs are deployed, or when ESSs are placed in nodes of the network providing little voltage support, no matter how big

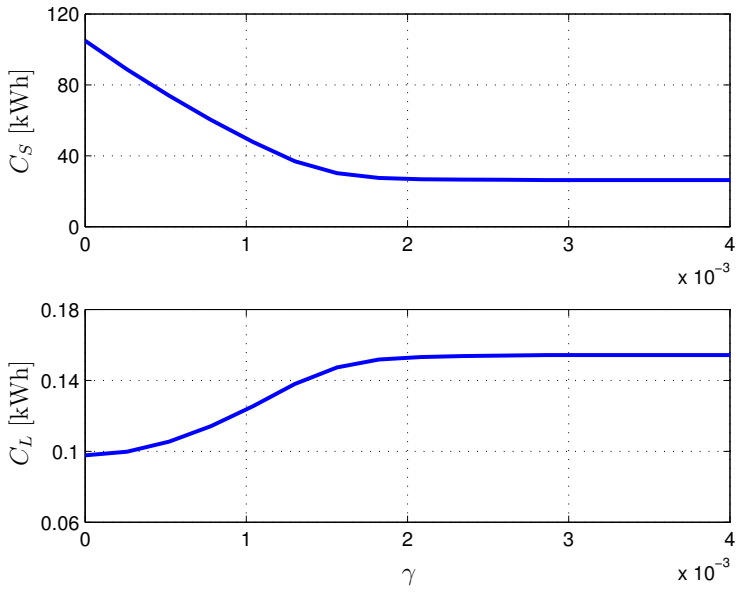

Fig. 5. Costs C_S and C_L at the optimum of problem (25) as a function of the weighting parameter γ for the IT-LV network. The set $\mathcal{S}$ is formed by ESSs placed at buses 7 and 11. Problem (25) is formulated over one challenging day of the data set, i.e. a day featuring both over- and undervoltages in the absence of ESSs.

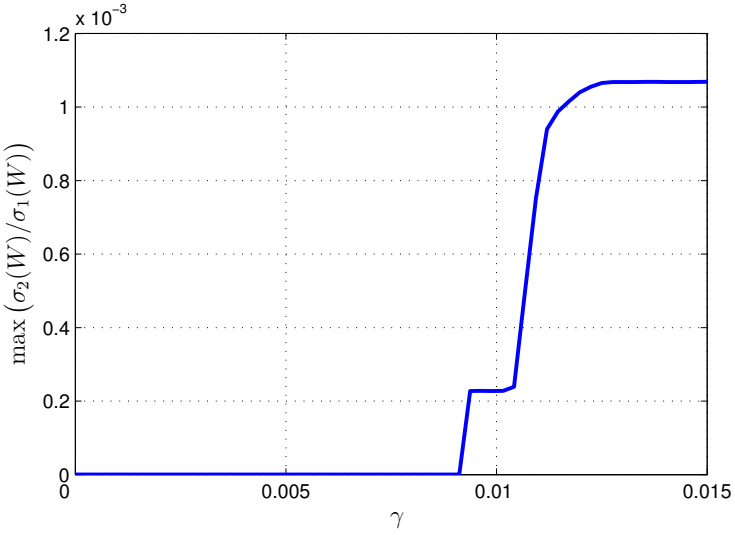

Fig. 6. Largest ratio of the second to the first singular value of $W(t)$, $t \in \mathcal{T}$, at the optimum of problem (25) as a function of the weighting parameter γ. The setting is the same as for Fig. 5.

the storage size is. If this is the case, the day for which problem (14) does not have a solution is termed *infeasible*. In practice, infeasible days are neglected when the average cost (32) and the final ESS sizes (26) are computed. However, the number of infeasible days provides useful information to make the final decision on ESS allocation.

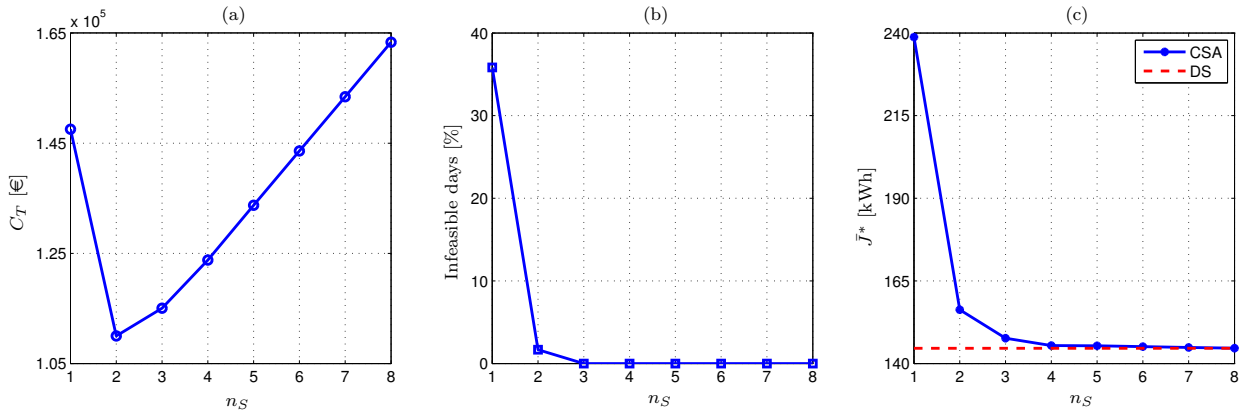

Fig. 7. Results of the proposed ESS allocation procedure for the IT-LV network. (a) Total deployment cost C_T in (31), where the expected value $\mathbf{E}[J^*]$ is replaced with the average cost $\bar{J}^*$ in (32). (b) Percentage of infeasible days. (c) Average cost $\bar{J}^*$ (blue solid line) and lower bound provided by the distributed allocation strategy (red dashed line).

The percentage of infeasible days as a function of n_S is shown in Fig. 7(b). It is apparent that a suitable choice is $n_S = 2$, corresponding to the minimum total deployment cost $C_T = 110$ k€, while the number of infeasible days is only 2 out of 120 (less than 2%). Notice in Fig. 7(a)-(b) that increasing the number of ESSs from one to two leads to a consistent reduction of both the total deployment cost and the infeasible days. On the other hand, further increasing n_S would zero out the infeasible days, but at the price of a significant cost increase. The average cost $\bar{J}^*$, used in place of the expected value $\mathbf{E}[J^*]$ in (31), is shown as a function of n_S in Fig. 7(c). In particular, for $n_S = 2$, $\bar{J}^* = 156$ kWh (this is the value $\bar{J}^*_{CSA}$ already reported in Section V-B). Notice that $\bar{J}^*$ tends to a constant value as n_S increases. Recalling (31), this explains why C_T in Fig. 7(a) grows linearly with n_S for $n_S \geq 4$.

D. Comparisons with Alternative Heuristics

In this section, the CSA algorithm is compared with other ESS allocation strategies. The Distributed Strategy (DS) consists of solving problem (25) for all the days in the data set under the assumption that a storage unit is available at each bus, i.e. $\mathcal{S} = \mathcal{N}^L$. Then, (26) is applied to determine the final ESS sizes. Since the optimal solution provided by DS is typically not sparse, i.e. $\hat{E}^*_s > 0$ for most $s \in \mathcal{N}^L$, the number of allocated ESSs is large, and hence the total deployment cost C_T is usually prohibitive (e.g., $C_T = 243$ k€ for the IT-LV network under consideration). Nonetheless considering DS is useful, since it provides a tight lower bound to (32), as can be observed in Fig. 7(c). The same figure shows that increasing n_S from one to two allows one to fill about 85% of the gap between the value of $\bar{J}^*$ provided by the CSA algorithm for $n_S = 1$ and the lower bound provided by DS. Moreover, the choice $n_S = 2$ results in a total ESS size $C_S = 64$ kWh which is slightly smaller than that provided by DS, namely 65 kWh (see Fig. 8, showing the sizes of the ESSs allocated at each bus by DS and by the CSA algorithm for $n_S = 2$).

The First Best Strategy (FBS) is based on DS. For a given number n_S of ESSs to be deployed, FBS builds the

set $\mathcal{S}_{FBS}$ of buses with ESS by taking the n_S buses with the largest sizes $\hat{E}_s^*$ in the solution provided by DS. Then, the optimal size of each ESS is computed by solving problem (25) with $\mathcal{S} = \mathcal{S}_{FBS}$ for all the days in the data set, and finally applying (26). For $n_S = 2$, buses 6 and 15 are selected by FBS to host the ESSs (see Fig. 8). The total deployment cost of this solution is $C_T = 111$ k€, with an average cost $\bar{J}^* = 157$ kWh. As can be observed, both FBS and the CSA algorithm achieve comparable results in terms of $\bar{J}^*$ and C_T for $n_S = 2$. This occurs also for different values of the weighting parameter γ in (13). However, FBS results in 11% of infeasible days for all $n_S \leq 6$. The reason for this lies in the fact that, as opposed to the CSA algorithm, FBS neglects the network topology, leaving the right-hand side of the network (see Fig. 1) without ESS for $n_S \leq 6$. Under the considered demand and generation data set, the feeder composed of the buses $\{8, 9, 10\}$ is likely to suffer from undervoltages. These cannot be solved with the solution provided by FBS until one chooses $n_S > 6$, thus introducing bus 10 in the set $\mathcal{S}_{FBS}$.

E. IEEE 34-Bus Case Study

The proposed ESS allocation procedure is validated on the IEEE 34-bus test feeder, by simulating demand and generation profiles of four days representative of the classes NV, UV, OV and UOV defined in Sec. V-B. As for the IT-LV network, the performance of the CSA algorithm is compared with the optimal solution for different numbers of ESSs to be deployed. The results for the four classes are summarized in Table II and confirm the effectiveness of the algorithm, with a maximum performance degradation smaller than 4%. With regard to computational aspects, for $n_S = 3$ the proposed procedure solves the siting and sizing problem for one day in approximately 18 minutes, almost totally required to solve problem (25). As expected, the computation time taken by the CSA algorithm is of the order of seconds irrespective of the number of buses, thus confirming that the siting procedure scales well with the network size. By contrast, the exhaustive search needed to compute the optimal ESS placement would require to solve 5456 problems of the form (25), implying an unacceptable computation time. For this reason, the exhaustive search needed to compute J_{OPT}^* is restricted to the set of the critical buses, which are the favourite ones for the ESS allocation.

By performing the same analysis illustrated for the IT-LV network, the total cost C_T is computed for different values of n_C and using the four-day data set. In this case, the optimal number of ESSs to deploy into the IEEE 34-

TABLE II

PERFORMANCE EVALUATION OF THE CSA ALGORITHM FOR THE IEEE 34-BUS TEST FEEDER (J_{CSA}^*/J_{OPT}^*).

n_S	NV	UV	OV	UOV
1	1.008	1.012	1.039	1.014
2	1.012	1.000	1.038	1.009
3	1.004	1.011	1.031	1.005

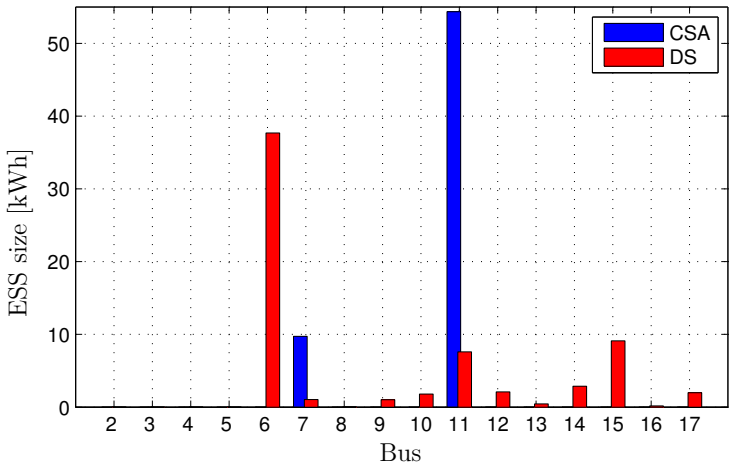

Fig. 8. Sizes $\hat{E}_s^*$ of the ESSs allocated by the distributed strategy (red) and by the CSA algorithm for $n_S = 2$ (blue) in the case of the IT-LV network.

bus system turns out to be $n_S = 1$, corresponding to a total cost $C_T = 52.8$ k€. According to the CSA algorithm, the location where to deploy the storage unit is bus 33, with an ESS size $C_S = 20.9$ kWh and an average cost $\bar{J}^* = 74.1$ kWh. For $n_S = 1$ FBS selects bus 19 as ESS location, achieving comparable performance ($C_T = 52.1$ k€, $C_S = 21.3$ kWh and $\bar{J}^* = 72.9$ kWh). However, the computation time of FBS, requiring the solution of (25) under the assumption that a storage unit is available at each bus, is remarkably larger.

F. Test on Random Networks

To further assess the effectiveness of our ESS allocation procedure, we run the CSA algorithm on 200 randomly generated radial networks and compare the results with the optimal ones obtained via exhaustive search. All networks are characterized by the same node set $\mathcal{N}$ as the IT-LV network (bus 1 being always the slack bus), but differ in the edge set $\mathcal{E}$ and the admittance matrix Y. The generation mechanism of the tree structure is recursive, starting from the slack bus as the root. Given a root node r and a set $\mathcal{L}$ of descendant nodes, m children c_i of r are randomly drawn from $\mathcal{L}$, where m ranges from 1 to 4 with equal probability. Then, the set of the remaining descendant nodes is randomly partitioned into m subsets $\mathcal{L}_i$. The same procedure is recursively repeated for each set $\mathcal{L}_i$ with root c_i, until the leaf nodes are reached. The depth of the 200 generated trees ranges from 3 to 7. Given the edge set $\mathcal{E}$, the admittance matrix Y is defined by generating randomly the distances between the nodes connected by an edge, and then multiplying the distances by a fixed admittance per unit length. On the other hand, demand and generation profiles are assumed to be a property of the buses (i.e. they are the same for all networks). The time step is 15 minutes, and the time horizon is one day, during which all the simulated networks feature over- or undervoltages at some buses.

For each network, the CSA algorithm is run with increasing values of n_C until it results in $n_S = 2$ deployed ESSs. Then, problem (25) is solved by assuming the corresponding ESS placement. Let J_{CSA}^* be the optimal cost

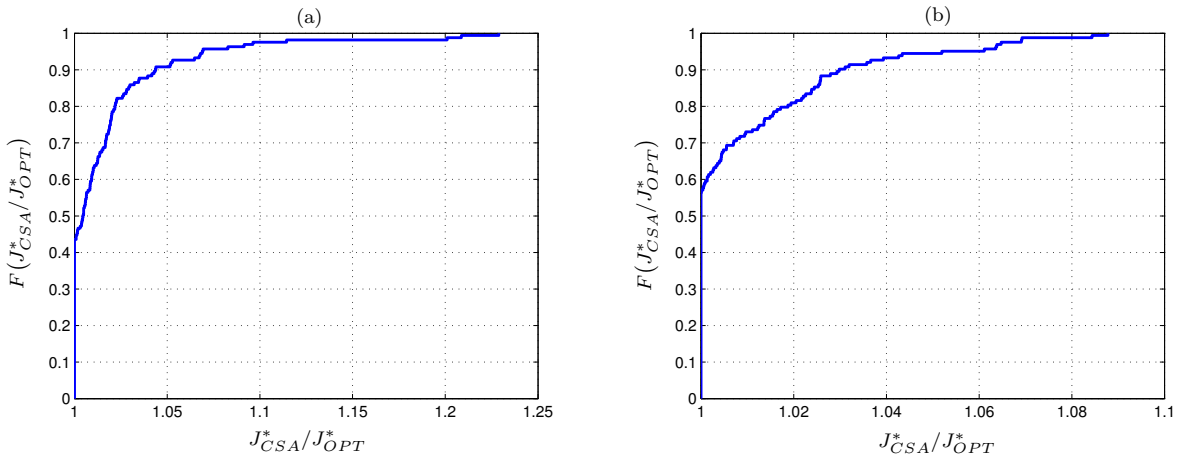

Fig. 9. Empirical distribution of the ratio J^*_{CSA}/J^*_{OPT} over 200 random networks equipped with (a) $n_S = 2$ and (b) $n_S = 3$ ESSs.

returned by (25) for that placement. Such a quantity is compared with the optimal cost J^*_{OPT}, computed over all possible placements of two ESSs in the network. The empirical distribution of the ratio J^*_{CSA}/J^*_{OPT} over the 200 networks is shown in Fig. 9(a). It can be noticed that the solution provided by the CSA algorithm is optimal in 45% of the cases, while only 9% of the cases reveal a degradation of the solution worse than 5%. Performance is even better when three ESSs are deployed, see Fig. 9(b): the solution provided by the CSA algorithm is optimal in 57% of the cases, while a degradation of the solution worse than 5% occurs only in 5% of the cases, with a maximum degradation of 8%.

The results, obtained by applying the ESS allocation procedure to random topologies, confirm the soundness of the intuition underlying the CSA algorithm.

VI. Conclusion

In this paper, a new method for designing the number, locations and sizes of energy storage systems, with the purpose of preventing over- and undervoltages in a LV network, has been proposed. In order to reduce the computational burden required by the solution of the resulting optimization problem, a heuristic procedure is devised. A voltage sensitivity analysis is proposed to circumvent the combinatorial nature of the siting problem. A multi-period OPF convex relaxation is adopted to determine the size of each storage unit. The procedure has been demonstrated on an Italian LV network, an IEEE test feeder and 200 randomly generated radial networks. The simulations show interesting results in terms of computation time and optimality of the solution found. Ongoing work is devoted to investigating suitable ESS control algorithms to be applied in real-time network operation.

References

[1] J. Tuominen, S. Repo, and A. Kulmala, "Comparison of the low voltage distribution network voltage control schemes," in *Proc. of 5th IEEE/PES Innovative Smart Grid Technologies Europe*, 2014, pp. 1–6.

[2] L. Wang, D. H. Liang, A. F. Crossland, P. C. Taylor, D. Jones, and N. S. Wade, "Coordination of multiple energy storage units in a low-voltage distribution network," *IEEE Transactions on Smart Grid*, vol. 6, no. 6, pp. 2906–2918, 2015.

[3] H. Nazaripouya, Y. Wang, P. Chu, H. R. Pota, and R. Gadh, "Optimal sizing and placement of battery energy storage in distribution system based on solar size for voltage regulation," in *Proc. of 2015 IEEE Power Energy Society General Meeting*, 2015, pp. 1–5.

[4] M. Nick, R. Cherkaoui, and M. Paolone, "Optimal siting and sizing of distributed energy storage systems via alternating direction method of multipliers," *International Journal of Electrical Power & Energy Systems*, vol. 72, pp. 33–39, 2015.

[5] U.S. Department of Energy, "Grid energy storage," [Online]. Available: http://energy.gov/oe/downloads/grid-energy-storage-december-2013 (accessed Apr. 27, 2016).

[6] Int. Electrotechnical Commission, "Electrical energy storage," [Online]. Available: http://www.iec.ch/whitepaper/pdf/iecWP-energystorage-LR-en.pdf (accessed Apr. 27, 2016).

[7] H. Pandzic, Y. Wang, T. Qiu, Y. Dvorkin, and D. S. Kirschen, "Near-optimal method for siting and sizing of distributed storage in a transmission network," *IEEE Transactions on Power Systems*, vol. 30, no. 5, pp. 2288–2300, 2015.

[8] M. Zidar, P. S. Georgilakis, N. D. Hatziargyriou, T. Capuder, and D. Škrlec, "Review of energy storage allocation in power distribution networks: applications, methods and future research," *IET Generation, Transmission & Distribution*, vol. 10, no. 3, pp. 645–652, 2016.

[9] K. A. Baker, "Coordination of resources across areas for the integration of renewable generation: Operation, sizing, and siting of storage devices," Ph.D. dissertation, Carnegie Institute of Technology, Carnegie Mellon University, 2014.

[10] M. Hoffman, M. Kintner-Meyer, J. DeSteese, and A. Sadovsky, "Analysis tools for sizing and placement of energy storage in grid applications," in *Proc. of ASME 5th International Conference on Energy Sustainability*, 2011, pp. 1565–1573.

[11] H. Zhao, Q. Wu, S. Huang, Q. Guo, H. Sun, and Y. Xue, "Optimal siting and sizing of energy storage system for power systems with large-scale wind power integration," in *Proc. of 2015 IEEE Eindhoven PowerTech*, 2015, pp. 1–6.

[12] C. Thrampoulidis, S. Bose, and B. Hassibi, "Optimal placement of distributed energy storage in power networks," *IEEE Transactions on Automatic Control*, vol. 61, no. 2, pp. 416–429, 2016.

[13] S. Wogrin and D. F. Gayme, "Optimizing storage siting, sizing, and technology portfolios in transmission-constrained networks," *IEEE Transactions on Power Systems*, vol. 30, no. 6, pp. 3304–3313, 2015.

[14] M. Ghofrani, A. Arabali, M. Etezadi-Amoli, and M. S. Fadali, "A framework for optimal placement of energy storage units within a power system with high wind penetration," *IEEE Transactions on Sustainable Energy*, vol. 4, no. 2, pp. 434–442, 2013.

[15] J. A. Taylor and F. S. Hover, "Convex models of distribution system reconfiguration," *IEEE Transactions on Power Systems*, vol. 27, no. 3, pp. 1407–1413, 2012.

[16] M. Nick, R. Cherkaoui, and M. Paolone, "Optimal allocation of dispersed energy storage systems in active distribution networks for energy balance and grid support," *IEEE Transactions on Power Systems*, vol. 29, no. 5, pp. 2300–2310, 2014.

[17] S. Bose, D. F. Gayme, U. Topcu, and K. M. Chandy, "Optimal placement of energy storage in the grid," in *Proc. of 51st IEEE Conference on Decision and Control*, 2012, pp. 5605–5612.

[18] D. Gayme and U. Topcu, "Optimal power flow with large-scale storage integration," *IEEE Transactions on Power Systems*, vol. 28, no. 2, pp. 709–717, 2013.

[19] M. Torchio, L. Magni, and D. Raimondo, "A mixed integer SDP approach for the optimal placement of energy storage devices in power grids with renewable penetration," in *Proc. of 2015 American Control Conference*, 2015, pp. 3892–3897.

[20] R. A. Jabr, S. Karaki, and J. A. Korbane, "Robust multi-period OPF with storage and renewables," *IEEE Transactions on Power Systems*, vol. 30, no. 5, pp. 2790–2799, 2015.

[21] S. Low, "Convex relaxation of optimal power flow – Part I: Formulations and equivalence," *IEEE Transactions on Control of Network Systems*, vol. 1, no. 1, pp. 15–27, 2014.

[22] P. Malysz, S. Sirouspour, and A. Emadi, "An optimal energy storage control strategy for grid-connected microgrids," *IEEE Transactions on Smart Grid*, vol. 5, no. 4, pp. 1785–1796, 2014.

[23] A. Giannitrapani, S. Paoletti, A. Vicino, and D. Zarrilli, "Algorithms for placement and sizing of energy storage systems in low voltage networks," in *Proc. of 54th IEEE Conference on Decision and Control*, 2015, pp. 3945–3950.

[24] J. Lavaei and S. H. Low, "Zero duality gap in optimal power flow problem," *IEEE Transactions on Power Systems*, vol. 27, no. 1, pp. 92–107, 2012.

[25] M. Brenna, E. De Berardinis, L. Delli Carpini, F. Foiadelli, P. Paulon, P. Petroni, G. Sapienza, G. Scrosati, and D. Zaninelli, "Automatic distributed voltage control algorithm in smart grids applications," *IEEE Transactions on Smart Grid*, vol. 4, no. 2, pp. 877–885, 2013.

[26] M. C. Nascimento and A. C. De Carvalho, "Spectral methods for graph clustering–a survey," *European Journal of Operational Research*, vol. 211, no. 2, pp. 221–231, 2011.

[27] J. P. Hespanha, "An efficient MATLAB algorithm for graph partitioning," [Online]. Available: http://www.ece.ucsb.edu/ hespanha/published/tr-ell-gp.pdf (accessed Apr. 27, 2016).

[28] W. Kersting, "Radial distribution test feeders," *IEEE Transactions on Power Systems*, vol. 6, no. 3, pp. 975–985, 1991.

[29] M. Grant and S. Boyd, "CVX: Matlab software for disciplined convex programming, version 2.1," [Online]. Available: http://cvxr.com/cvx (accessed Apr. 27, 2016).

[30] J. Sturm, "Using SeDuMi 1.02, A Matlab toolbox for optimization over symmetric cones," *Optimization Methods & Software*, vol. 11, no. 1-4, pp. 625–653, 1999.